# Intermolecular protein interactions in solutions of bovine lens $\beta_L$-crystallin

## Results from $1/T_1$ nuclear magnetic relaxation dispersion profiles

S. H. Koenig,* R. D. Brown III,* A. K. Kenworthy,‡ A. D. Magid,‡ and R. Ugolini*

*IBM T. J. Watson Research Center, Yorktown Heights, New York 10598; and ‡Department of Cell Biology, Duke University Medical Center, Durham, North Carolina 27710 USA

ABSTRACT We report the magnetic field dependence of $1/T_1$ of solvent water protons and deuterons (nuclear magnetic relaxation dispersion, or NMRD, profiles) for solutions of steer lens $\beta_L$-crystallin. Such data allow the study of intermolecular protein interactions over a wide concentration range, here 1–34% vol/vol, by providing a measure of the rotational relaxation time of solute macromolecules. We conclude that, for ≤5% protein, the solute particles are noncompact, with a rotationally averaged volume approximately three times that of a compact 60-kD sphere. (Earlier results for $\alpha$-crystallin, ~1,000 kD, from optical and osmotic measurements (Vérétout and Tardieu, 1989. *J. Mol. Biol.* 205:713–728), show a similar, approximately twofold, effect.) At intermediate concentrations, to ~20% protein, there is evidence for limited association or oligomerization, as found for the structurally related $\gamma_{II}$-crystallin (Koenig et al. 1990. *Biophys. J.* 57:461–469), to a limiting size about two-thirds that of $\alpha$-crystallin. The difference in NMRD behavior of the three classes of crystallins is consonant with their differing osmotic properties (Vérétout and Tardieu. *J. Mol. Biol.* 1989. 205:713–728; Kenworthy, McIntosh, and Magid. *Biophys. J.* 1992. 61:A477; Tardieu et al. 1992. *Eur. Biophys. J.* 21:1–12). We indicate how the unusual structures and interactions of these three classes of proteins can be combined to optimize transparency and minimize colloid osmotic difficulties in eye lens.

## INTRODUCTION

The refractive and transmissive properties of mammalian eye lens depend on the presence of high concentrations of $\alpha$-, $\beta$-, and $\gamma$-crystallins, broad classes of proteins that vary in size over several orders of magnitude and whose evolutionary relationships are becoming better understood (1-3). All mammalian crystallins have unusual interactive properties in solution, particularly at high concentrations (4), ostensibly needed both to minimize gradients of osmotic pressure that would otherwise accrue from radial gradients of crystallin concentration in lens (5-10) and to maximize lens transparency (10).

Solute $\alpha$-crystallin molecules are the largest crystallins (~1,000 kD (11)). At high concentrations, their osmotic pressures (10) are greater than the "ideal" values obtained using a hard sphere model, including higher order virial corrections (12), if it is assumed that the solute molecules are compact. Consistent with this, a successful first order description of both x-ray scattering and osmotic effects can be had by assuming that solute $\alpha$-crystallin molecules are noncompact hard spheres with an excluded volume somewhat over twice that of compact hard spheres of the same protein mass (when computed using a partial specific volume of 0.73 $cm^3/g$) (10).

The several $\gamma$-crystallins are the smallest crystallins (~20 kD (13)). In contrast to $\alpha$-crystallin, a solution of mixed $\gamma$-crystallins has a larger osmotic pressure at low concentrations (as expected from the lower molecular weight) which, however, increases only slightly with increasing protein concentration; the osmotic pressures of $\alpha$- and $\gamma$-crystallin solutions become equal at ~30% by weight (9). This has been attributed, on the one hand, to an attractive intermolecular interaction in solutions of mixed (9) and separated (14) $\gamma$-crystallins and, on the other hand, to extensive oligomerization until the solute molecules (for $\gamma_{II}$-crystallin) approach the size of solute $\alpha$-crystallin (6). On either view, there is a fundamental difference in the osmotic behavior of $\alpha$- and $\gamma$-crystallins. However, for both, particularly at high concentrations, their interprotein interactions are far different from what can be modeled by compact spheres that only interact upon contact.

The $\beta$-crystallins, oligomers of several related acidic and basic subunits (15-17), are intermediate in size between $\gamma$- and $\alpha$-crystallins. The $\beta$ subunits are relatively small (~27 kD) and structurally similar to $\gamma_{II}$-crystallin (3, 18, 19). $\beta$-crystallins account for over 40% of the crystallins in the bovine lens (with ~40% $\alpha$-crystallin in cortical and ~21% in nuclear extracts (see reference 9)). Separation of lens crystallins by size-exclusion chromatography typically yields two $\beta$-crystallin weight classes, $\beta_L$-crystallin and $\beta_H$-crystallin (for "light" and "heavy," respectively), although under certain conditions greater separation has been obtained (20-22). A weight-average molecular weight of 59 kD was estimated for $\beta_L$-crystallin (23) from sedimentation equilibrium measurements of dilute solutions. Recently, osmotic pressure-concentration isotherms for calf cortical $\beta$-crystallin (14) and steer $\beta_L$-crystallin have been reported (24, 25). The osmotic data for steer $\beta_L$-crystallin are similar to those for hemoglobin (26) (of comparable molecular weight), and can be modeled over the range 0.03–0.30 $gm/cm^3$ by the (nonlinear) behavior of compact hard spheres of

Address correspondence to Seymour H. Koenig, IBM T. J. Watson Research Center, Yorktown Heights, NY 10598.


0006-3495/93/04/1178/09 $2.00

80 kD (Kenworthy, Magid, and McIntosh, manuscript in preparation).

We report the magnetic field dependence of the longitudinal magnetic relaxation rate $1/T_1$ of solvent deuterons and protons in water solutions (known as $1/T_1$ NMRD or nuclear magnetic relaxation dispersion profiles) of bovine $\beta_L$-crystallin. Proton relaxometry measurements are among the few experimental approaches available for studying interprotein interactions and oligomerization over a wide range of protein concentration, used here for 1–34% solute vol/vol. Deuteron data must often be restricted to the lower one-third of this concentration range to keep $1/T_1$ from becoming too large to measure accurately on our system. $1/T_1$ of solvent water nuclei in the presence of diamagnetic globular protein solute decreases monotonically with increasing field, with an inflection—determined by the rotational relaxation time $\tau_R$ of solute macromolecules—from which the molecular weight of compact spherical proteins can be inferred (27–29). For deuterons, the profiles arise solely from alterations of the molecular dynamics of solvent water at the solute-solvent interface (30), and should, in principle, yield the more reliable values for $\tau_R$. (For protons, there is an additional effect, which involves transfer of Zeeman energy across the solute-solvent interface. The extent of this transfer contribution, and its dependence on field, are determined by the mechanism of diffusion of Zeeman energy within the solute protein, which in turn depends on $\tau_R$; this can distort the form of the proton NMRD profiles somewhat and make the absolute values obtained for $\tau_R$ less reliable (31).) Qualitative changes in the form of the proton $1/T_1$ profiles occur near ~50,000 kD (see reference 29). Below this value, Brownian rotation of solute protein is sufficiently rapid for proton relaxation to be liquid-like; at higher weights, it becomes solid-like. We will call these "mobile" and "immobile" protein systems respectively.

Previous papers have reported proton $1/T_1$ NMRD studies of calf lens homogenates (32–34), purified calf $\gamma_{II}$-crystallin (5, 6), and cortical and nuclear calf $\alpha$-crystallin (35). Common to all these systems are transitions, when the solute concentration exceeds ~15% protein vol/vol, from mobile to immobile behavior. These transitions are characterized, not only by a change in functional form of the profiles (discussed critically for $\alpha$-crystallin (35)), but by the appearance, at higher concentrations, of spectra-like features ($^{14}N$ peaks, most visible between 2 and 3 MHz) known to arise from cross-relaxation (magnetization transfer of Zeeman energy) between solvent protons and the $^{14}N$ nuclei of backbone NH moieties (36–40). It was argued, particularly for $\gamma_{II}$-crystallin, that the common transition near 15% protein vol/vol (about equal to the solids content of blood and most tissues) relates to a need to minimize osmotic problems in vivo while achieving lens function. Colloid osmotic pressure of protein solutions (when approximated by hard spheres) depends on both the number and excluded volume of solute particles (12). Increase in particle molecular weight due to rapidly increasing association with increasing concentration could make the osmotic pressure relatively insensitive to concentration by scaling down both components. Such osmotic behavior has been reported for $\gamma$-crystallin mixtures (9, 14), and attributed to oligomerization (6), but is not exhibited by $\alpha$-crystallin (10).

Calf $\gamma_{II}$-crystallin, with a monomer of ~20 kD, has an unusual, essentially unique, dependence of solute size on concentration in solution below the 15% transition, as inferred from NMRD results. It begins to oligomerize at relatively low concentrations, the more so the lower the temperature; with increasing concentration, oligomerization increases the average size of the solute macromolecular entities from the 20 kD monomer value to ~30 kD at 3% and ~300 kD at 15% vol/vol $\gamma_{II}$-crystallin at 35°C, at which point the reversible transition occurs that induces $^{14}N$ peaks (6). For $\alpha$-crystallin, by contrast, the molecular weight derived from NMRD data is relatively independent of concentration and temperature, 1,350–1,700 kD, assuming the solute molecules relatively compact and spherical, a range of values consistent with other findings (10) that the solute occupies about twice the volume that a compact protein would. Within this framework, the NMRD behavior of $\alpha$-crystallin and $\gamma_{II}$-crystallin is consistent with what is known of their molecular weights, and with the few other data, notably osmotic pressure (10), which compare these two protein classes over a wide range of concentration.

The present work, the first to combine deuteron and proton NMRD studies to characterize interprotein interactions, examines the behavior of $\beta_L$-crystallin, of intermediate molecular weight. These studies can be expected to answer the following questions: Does $\beta_L$-crystallin exhibit the mobile-immobile transition, as indicated by $^{14}N$ peaks? If so, is its onset in the same concentration range as found for other crystallin preparations? As found for the structurally related $\gamma_{II}$-crystallin, does $\beta_L$-crystallin oligomerize below the transition concentration? And, can the NMRD profiles of this protein be related to its osmotic properties over a wide concentration range?

## MATERIALS AND METHODS

### Bovine $\beta_L$-crystallin

Eyes from 18–24-mo-old steers were freshly harvested at slaughter and transported to the laboratory on ice. All further procedures were carried out at room temperature. From decapsulated lenses, cortical tissue (the outer 50% by weight) was separated and extracted, in two volumes of buffer, in a motor-driven glass-Teflon homogenizer. Extracts were clarified by centrifugation (20,000 *g* for 30 min), applied to a size-exclusion column (100 × 2.5 cm) containing Sepharose CL-6B, and eluted at 8–10 cm/h. The buffer for homogenation and elution was 50 mM NaCl, 50 mM Tris · HCl, 1 mM EDTA, 5 mM $NaN_3$, pH 7.6. Pooling of $\beta_L$-crystallin fractions was guided by analysis using discontinuous sodium dodecyl sulfate-polyacrylamide gel electrophoresis on slab gels. $\beta_L$-crystallin fractions were concentrated to ~0.1 g/ml by ultrafiltration, using an Amicon device with 10 kD cut-off membranes, and concentrated further in dialysis bags packed in dry Sephadex G-25. Dilution to intermediate protein concentrations was with the buffer augmented to 150 mM NaCl and 0.2 mM dithiothreitol (DTT), and the pH lowered to 6.8.

Initial and final protein concentrations (g/ml) were determined by refractive index measurements using a specific refractive increment of 0.187 ml/g (8). Concentrations are given throughout in volume fraction of protein, obtained from the concentration in units of g/ml of solution multiplied by 0.73 $cm^3/g$, the partial specific volume of protein. This is done for ease of comparison with NMRD results for other crystallins, and should not be confused with the total volume excluded by solute (as used, e.g., in computing osmotic pressure); the two quantities are equal only if the solute particles are compact, incorporating little water within their structure.

## Measurement and interpretation of NMRD profiles

$1/T_1$ of solvent water protons can be measured at any value of magnetic field over the range 0.01–50 MHz proton Larmor frequency, corresponding to 0.00024–1.2$T$, with an automated field-cycling relaxometer developed at IBM (41). For deuterons, with a gyromagnetic ratio lower by a factor 1/6.5, the accessible field range is in principle 0.0015–7.5 MHz deuteron Larmor frequency. For technical reasons, the highest measuring field used here was 5.4 MHz. The relaxometer can be set to detect either deuterons or protons by adjusting the resonance field during the appropriate part of the cycle to resonate either nucleus at 7.5 MHz. The initial magnetization of the deuteron spin system is also sixfold lower than for protons, which reduces signal intensity by the same factor. Finally, deuteron relaxation rates are intrinsically greater than proton rates by an order of magnitude for comparable circumstances (in diamagnetic systems), which can increase significantly the amount of signal lost while waiting for the magnetic field to switch and stabilize (42). These several factors can only be partially overcome by repeating data points, so that the NMRD profiles for deuterons are, in general, noisier and less accurate than those of protons for reasonable data acquisition times.

A sample, in a stoppered test tube, is surrounded by freon in contact with chamber walls maintained at fixed temperature with a circulating water-ethylene glycol mixture, allowing measurements in the range −8 to 35°C, with the temperature regulated to within ±0.2°C in order to stabilize relaxation rates to within the uncertainty of ±1% with which they can generally be measured (for protons).

Measurements of deuteron and proton $1/T_1$ NMRD profiles, both of which yield the rotational relaxation time $\tau_R$ of compact macromolecular solute, have proven to be particularly useful for studying interactions of diamagnetic globular proteins in solution. Details and references are given in earlier papers of this series (see references 6, 35). In short, the data are fit to the four-parameter Cole-Cole expression (43) to characterize the monotonic parts of the NMRD profiles, both for the information they contain and to use as a subtractive background so that the structured regions of proton profiles can be expanded. Rewritten for $1/T_1$ NMRD data, it becomes, for deuterons and protons (28):

$$\frac{1}{T_1} = \frac{1}{T_{1w}} + D + A(\nu_c)Re\left(\frac{1}{1 + (i\nu/\nu_c)^{\beta/2}}\right), \qquad (1)$$

where $Re$ means "the real part of", $1/T_{1w}$ is the contribution of solvent, $D$ and $A$ (which is a function of $\nu_c$) are the respective amplitudes of a high field limiting and a low field dispersive contribution to the NMRD profile, and $\nu$ is the Larmor frequency. The curve has an inflection point (which corresponds to the half-amplitude point of the dispersive component) at $\nu/\nu_c = 1$; $\beta$ is a parameter that determines the slope of the profile at the inflection. $\beta = 2$ gives a Lorentzian; its value for proton NMRD profiles of most globular proteins is in the range 1.4–1.7 (28). $1/\nu_c$ is proportional to $\tau_R$, here taken to be the time appropriate for relaxation of interactions with the symmetry of second rank tensors, i.e., $d$-like symmetry; this is one-third the Debye value, which is for $p$-like symmetry. In light of recent work (30), which has established that solvent senses the rotation of protein by exchange of hydration waters with a residence lifetime $\tau_{hy} \simeq 1$ μs, the usual relation between $\nu_c$ and $\tau_R$ (see reference 35) must be altered somewhat to include $\tau_{hy}$. It then becomes convenient to define a correlation time $\tau_c$ such that

$$1/\nu_c \equiv 2\pi(\sqrt{3})\tau_c = 10.9\tau_c, \qquad (2a)$$

where, for spherical proteins (27, 29),

$$\frac{1}{\tau_c} \simeq \frac{1}{\tau_R} + \frac{1}{\tau_{hy}}; \quad \tau_R = 4\pi\eta r^3/3kT. \qquad (2b)$$

Here $r$ is the radius of the hydrated solute protein (assumed spherical but not necessarily compact), $T$ is the absolute temperature, and $\eta$ is the (temperature dependent) microscopic viscosity as experienced by the solute particles. The inclusion of $\tau_{hy}$ becomes relevant only at high concentrations of $\beta_L$-crystallin, when $\tau_R \gtrsim \tau_{hy}$, corresponding to an effective molecular weight $\gtrsim$ 3,500 kD. The effective particle size can increase another order of magnitude with no change in $\tau_c$, until the transition to immobile behavior sets in and the form of the profile changes.

For proteins that are nonspherical, but approximately ellipsoidal, $\tau_R$ (as derived from $\nu_c$) is a complex average which, however, differs little from that of a sphere of the same volume unless the protein is highly anisotropic, $\gtrsim$2:1 axial ratio (44, 45). ($\tau_R$ is independent of the density of the solute particle, so long as its mass distribution is uniform.) For proteins of more complex shape, e.g., approximated by an hour-glass, one expects that $\tau_R$ would be close to that of a hydrodynamically equivalent sphere defined by rotational averaging of the space occupied by a protein molecule. In the dilute limit, $\eta$ is equal to $\eta_0$, the viscosity of the neat solvent. The ratio $\eta/\eta_0$ increases with protein content due to hydrodynamic effects, only becoming significant in the present context for $\gtrsim$20% protein (46). The dependence of $\nu_c$ on viscosity, temperature, and protein size has been well studied and amply verified for protons (see Fig. 2 of reference 29). The result is molecular weight (kD) $\simeq 350/(\nu_c(\text{MHz}))$ at 25°C, although this approximation overestimates the mass of lighter proteins somewhat (see reference 29). For deuterons, the results are similar, although the data are less extensive.

Notwithstanding the experimental difficulties, deuteron $1/T_1$ NMRD profiles are intrinsically more accurate for comparing protein molecular weights than are proton profiles because the former are generated only by Brownian rotation of solute and its influence on the relaxation rates of specific bound water molecules (30), whereas the detailed form of $1/T_1$ proton profiles (including $\nu_c$) are affected by magnetization transfer (31). For proteins of the molecular weight range of interest here, one has the particular advantage that essentially the entire major NMRD dispersion can be obtained by observing deuterons; hence the emphasis below on deuteron NMRD profiles.

From relaxation theory, the product $A\nu_c$ should have no explicit dependence on $\nu_c$, although $A$ has an implicit dependence on $\nu_c$. When expressed in terms of $A_R$, the value of the $A$-term per millimole of solute (the relaxivity), the product $A_R\nu_c$ is found to be linear in molecular weight (28, 29). (A naive expectation would be that $A_R$ is proportional to the protein surface area, or weight$^{2/3}$.) For protons, the data give (see Fig. 4 of reference 29) $A_R \simeq 9.4 \times 10^{-5} \times$ (molecular weight (kD))$^2$. Finally, below ~20% protein by volume, $A_R$ can be taken to be independent of concentration (6) for noninteracting solute molecules; at higher concentrations, effects of one solute molecule on the hydrodynamics of another cannot be neglected.

The utility of the Cole-Cole description for analyzing the $1/T_1$ NMRD profiles of globular protein solutions is that the empirical relations among molecular weight, $\nu_c$, and $A_R$ are satisfied by at least one dozen proteins (29) ranging over almost three decades in molecular

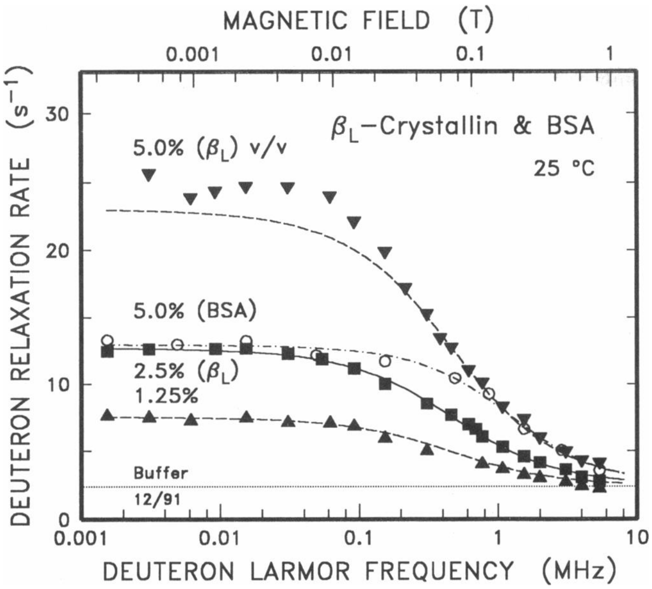


FIGURE 1 Deuteron $1/T_1$ NMRD profiles of steer $\beta_L$-crystallin, 5% (▼), 2.5% (■), and 1.25% (▲) vol/vol, and 5% vol/vol bovine serum albumin (BSA) (○), at 25°C. The solid curve through the data points for the 2.5% sample, and the dot-dashed curve through the BSA data, derive from least squares comparisons of the data with the Cole-Cole expression, Eq. 1. The dashed curves associated with the 1.25 and 5% $\beta_L$-crystallin profiles were obtained by scaling the solid curve by the factors 0.5 and 2, respectively (correcting appropriately for the buffer background indicated). The excellent agreement with the 1.25% data indicates no change in solute association between the two concentrations; the ~12% difference for the 5% data suggests a small, but not significant, increase in association at the higher concentration. The more than four-fold higher value inflection field of the (68 kD) BSA profile indicates that the molecular weight of $\beta_L$-crystallin, assuming it is compact and reasonably spherical, is greater than that of BSA by this factor (see text).

weight; significant deviations from such behavior are thus indicative of anomalies in protein conformation and interactions in solution.

## RESULTS AND ANALYSES

### Low-concentration-range molecular weight of $\beta_L$-crystallin: deuteron profiles

Fig. 1 shows deuteron $1/T_1$ NMRD profiles of $\beta_L$-crystallin at three relatively low protein concentrations (5 (▼), 2.5 (■), and 1.25% (▲) vol/vol) obtained by successive dilution. The buffer contribution is also shown. The solid curve through the 2.5% profile results from a Cole-Cole fit with $\nu_c = 0.51$ MHz. (A fit to the 5% profile gives $\nu_c = 0.36$ MHz, which is the more accurate because of the higher rates.) The dashed curves associated with the other $\beta_L$-crystallin profiles were generated by scaling the solid curve by the respective concentration ratios (with appropriate corrections for the buffer contribution). These curves should match the data points, assuming no dilution errors and no change in average solute mass with concentration. The results indicate little concentration-dependent mass change, with an increase ~12% in the average $\tau_R$ at 5% protein, judged from the difference in the magnitudes of the low field rates.

To estimate the mass of $\beta_L$-crystallin (more properly, a mean hydrodynamic value of $\tau_R$), a deuteron profile of 5% bovine serum albumin (BSA, 68 kD) was measured. BSA is a well behaved protein, and much data for both the deuteron and proton profiles have been obtained, with identical values of $\nu_c$ obtained for each (30), and close to the value for hemoglobin, which has essentially the same molecular weight. The BSA profile is also shown in Fig. 1 (○); the Cole-Cole fit gives $\nu_c = 1.65$ MHz, a factor 4.6 greater than the results for the 5% crystallin data. Thus, as sensed by deuterated solvent, and using the orientational relaxation rate of BSA as a standard, the molecular weight of $\beta_L$-crystallin, for the solvent conditions of Fig. 1, is ~300 kD. That is, solute $\beta_L$-crystallin molecules reorient by Brownian rotation at a rate equivalent to compact spherical protein of 300 kD. Extrapolation of the proton data to the dilute limit (see below) lowers this value to 200 kD, whereas any correction for the known asphericity of BSA increases this value. The increase is somewhat difficult to compute since the orientations of all the hydration waters that contribute to relaxation must be known (see Fig. 2 of reference 44); for BSA, with axial ratio ~ 2.9, one can estimate a factor ~ 1.5, assuming the waters randomly oriented.

### Low-concentration-range molecular weight of $\beta_L$-crystallin: proton profiles

Proton $1/T_1$ NMRD profiles were obtained over a wide range of $\beta_L$-crystallin concentration, with the results of Cole-Cole analyses given in Table 1. It is clear that $\nu_c$ decreases monotonically with increasing concentration. A plot (not shown) of $1/\nu_c$ (proportional to solute size, Eq. 2b) is linear below 15% protein; extrapolation to zero protein concentration gives 0.63 MHz, or a factor 1.5 higher than $\nu_c$ at 5% protein. Applying this factor to

**TABLE 1 Proton cole-cole parameters for $\beta_L$-crystallin at 25°C: comparison with cortical $\alpha$-crystallin (parentheses) (35)**

| Concentration | $A$ | $D$ | $\beta$ | $\nu_c$ |
|---|---|---|---|---|
| *% vol/vol* | $s^{-1}$ | $s^{-1}$ | | *MHz* |
| 34 | 103 | 1.3 | 1.2 | ~0.12 |
| 30 | 83 | 1.1 | 1.2 | 0.13 |
| 25 (24) | 54 (56) | 0.81 | 1.2 (1.1) | 0.15 (0.086) |
| 20 (20) | 35 (37) | 0.48 (0.7) | 1.2 (1.2) | 0.19 (0.13) |
| 15 (15) | 21 (24) | 0.30 (0.5) | 1.2 (1.2) | 0.25 (0.15) |
| 10 (10) | 11 (13) | 0.07 (0.38) | 1.2 (1.3) | 0.29 (0.21) |
| 7.5 | 7.5 | 0.02 | 1.2 | 0.34 |
| 5 (5) | 4.5 (5.3) | ~0 (0.18) | 1.2 (1.4) | 0.40 (0.26) |
| 3.5 | 2.9 | ~0 | 1.2 | 0.44 |
| 1.75 | 1.2 | ~0 | 1.2 | 0.52 |
| 1 | 0.63 | ~0 | 1.2 | ~0.4 |

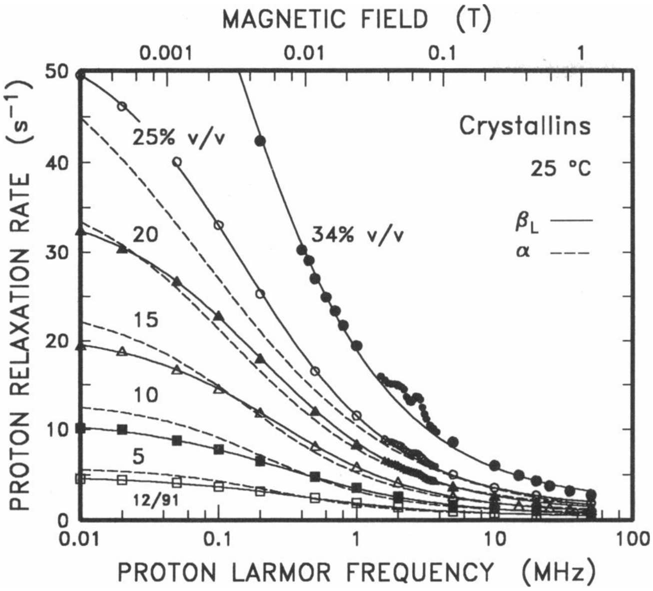


FIGURE 2 Proton $1/T_1$ NMRD profiles of steer $\beta_L$-crystallin, at 25°C, for 34% (●), 25% (○), 20% (▲), 15% (△), 10% (■), and 5% (□) vol/vol protein. The solid curves through the data points derive from a least squares comparison of the data, excluding all structure in the 1–4 MHz region, with the Cole-Cole expression, Eq. 1. The dashed curves are similar fits to cortical α-crystallin, also at 25°C (35).

the deuteron data of Fig. 1, as noted, gives the estimate for the effective molecular weight of $\beta_L$-crystallin, in the dilute limit, of ~200 kD. Note that this is a value related to the orientational relaxation time of a compact sphere of this mass; this could be reconciled with a lower molecular weight if the solute protein were spherical but not compact, or had a more complex shape, e.g., approximated by an ellipsoid or an hour-glass. For comparison, a sphere which would just enclose the βB2 homodimer unit cell (47) would have a molecular weight of 215 kD, if composed of compact protein.

## High-concentration range of $\beta_L$-crystallin: proton profiles and comparison with α-crystallin

In Fig. 2, the proton $1/T_1$ NMRD profiles of $\beta_L$-crystallin and earlier cortical α-crystallin data (35) are compared for concentrations ≥ 5% vol/vol protein. The respective Cole-Cole parameters are given in Table 1. Several concentrations of steer α-crystallin prepared from the same homogenates as the $\beta_L$-crystallin used here gave profiles (unpublished data) in agreement with the published results for calf α-crystallin (35). For 10–20% protein, Fig. 2 and Table 1, $\beta_L$-crystallin behaves as if it were somewhat lighter than, but otherwise similar to, α-crystallin. The average ratio of $\nu_c$ values is 1.5, and that of $A$ is 0.83.

There are several qualitative inferences that can be drawn from the results in Table 1. For example, throughout the range, β (which relates to the slope of the NMRD profiles at $\nu_c$) for $\beta_L$-crystallin is relatively constant at 1.20, whereas that of α-crystallin decreases with increasing concentration. (Recall that $\beta = 2$ corresponds to a Lorentzian profile and arises from a mechanism that can be characterized by a single correlation time. Since the data are represented on a semilogarithmic plot, a sizable spread of correlation times, from a superposition of mechanisms, will look "quasi-Lorentzian," with $\beta < 2$.) As the $\beta_L$-crystallin profiles have obvious inflections, the consistent low values of β suggest a limited spread of correlation times about an identifiable mean value, which could result from a significant shape anisotropy of the solute particles. Such an anisotropy would also increase the surface area for a given molecular weight, and thereby the number of water-binding sites. This would give a somewhat larger intrinsic value of $A$ for $\beta_L$-crystallin than for α-crystallin (after adjustment for the different $\nu_c$ values), as seen in Table 1 for 10–25% protein.

As another example, the values of β suggest that $\beta_L$-crystallin solute particles do not reach the very large (solid-like) size (i.e., large values of $\tau_R$) found for α-crystallin (35), i.e., do not become as rotationally immobile as α-crystallin molecules for a given high protein concentration. (Recall that, for α-crystallin at high concentration, the long $\tau_R$ arises from enhanced interprotein interactions because of their noncompact solute structure.) This lesser interaction for β-crystallin is evidenced by the facts that the Cole-Cole parameter β does not continue to decrease, that a realistic value for $\nu_c$ can be obtained even for the highest protein concentration, and that the structured region varies more slowly with concentration than for other crystallins (see below). More specifically, from the data for the 25% sample, Fig. 2 and Table 1, using Eq. 2, a and b, $\nu_c = 0.15$ MHz corresponds to $1/\tau_R = 0.06$ MHz, the rotational relaxation time of a 9,000 kD spherical equivalent protein. This is about fivefold below the mobile-immobile transition and, accordingly, peaks for this sample are barely apparent. Increasing concentration to 34%, for which the data do not provide a good measure of the increased $\nu_c$, show the peaks clearly.

## $^{14}$N peaks of $\beta_L$-crystallin and other crystallins

The $^{14}$N peaks of $\beta_L$-crystallin are shown on an expanded scale in Fig. 3 (●), along with analogous published results for other crystallin preparations. The upper (▽) and lower (△) data are from preparations of calf cortical lens homogenates, concentrated and native, respectively (32). These data quite closely span the range of the phenomena, as well as indicate the sensitivity of the magnitude of the peaks to protein concentration. A fourth profile, for 24% α-crystallin (□), is also shown. Except for the absence of structure near 1 MHz, the $^{14}$N spectra for $\beta_L$-crystallin do not differ substantively from those of the other preparations, although a higher concentration is required for a given rate. A comparison of the 2.8 MHz

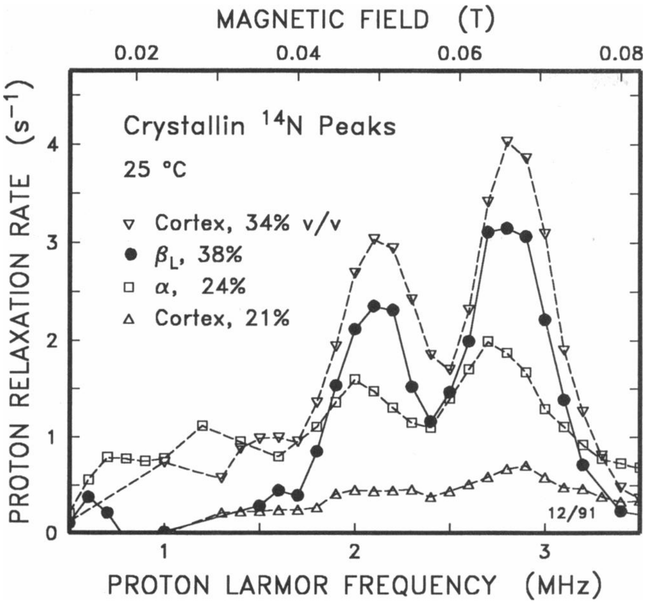


FIGURE 3 [14]N peaks (expanded) in the proton $1/T_1$ NMRD profiles for 38% vol/vol $\beta_L$-crystallin, from the present work (●); for 24% bovine cortical α-crystallin (□) (after 35); and 34% (▽) and 21% (△) calf cortical homogenate (after 32), all at 25°C.

[14]N peak of $\beta_L$-crystallin with a wider range of crystallin preparations is shown in Fig. 4. It may be of note that, for $\beta_L$-crystallin, the dependence of osmotic pressure on concentration changes in functional form above ~21% protein (Kenworthy, Magid, and McIntosh, manuscript in preparation), near the onset of the [14]N peaks, Fig. 4.

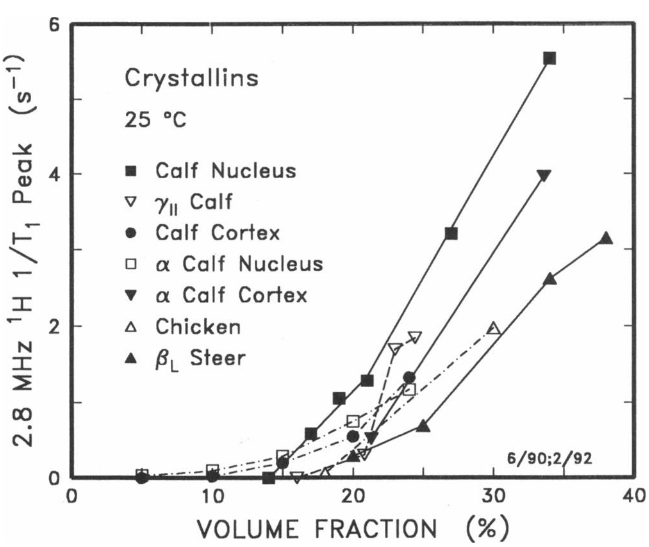


FIGURE 4 Height of the 2.8 MHz [14]N peak above the monotonic background, at 25°C, for steer $\beta_L$-crystallin (▲) as a function of volume fraction of protein (present work) compared with analogous data for other preparations: calf nuclear (■) and cortical (●) (32); calf $\gamma_{II}$-crystallin (▽) (6); calf nuclear (□) and cortical (▼) α-crystallin (35); and chicken homogenate (△) (32). The volume fraction was obtained in each case by multiplying the known weight fraction by 0.73.

**TABLE 2 Proton cole-cole parameters for $\beta_L$-crystallin at 5°C**

| Concentration | $A$ | $D$ | $\beta$ | $\nu_c$ |
|---|---|---|---|---|
| *% vol/vol* | $s^{-1}$ | $s^{-1}$ | | *MHz* |
| 20 | 58 | 1.1 | 1.3 | 0.13 |
| 5 | 7.1 | 0.05 | 1.3 | 0.30 |
| 3.5 | 4.7 | 0.02 | 1.3 | 0.34 |
| 1.75 | 2.0 | 0.04 | 1.3 | 0.39 |
| 1 | 1.1 | ~0 | 1.2 | 0.41 |

At present, the theory of [14]N peaks, including their temperature dependence, is rather rudimentary (39, 40); a major indication is that peaks of the magnitude plotted in Fig. 3 require that the magnetization of solute protons be in magnetic contact with the majority of protein NH protons. Whether this is dominated by direct contact through chemical diffusion of solvent or magnetization transfer at the protein-solvent interface and spin diffusion within the protein is an unsettled issue at present, although there is increasing evidence that magnetization transfer dominates (48, 49).

## Temperature effects

The experiments of Fig. 2 were repeated at 5°C for several samples with ≲20% protein; analyses of the data gave the results in Table 2. Of particular note is that nothing untoward occurs; the changes in the $A$-term and in $\nu_c$ on going from 25 to 5°C are those expected from changes in the neat solvent viscosity in a solution of protein particles of temperature independent mass, as found previously for α-crystallin (35). The major distinction between the behavior of the two crystallins at the two temperatures is that, for $\beta_L$-crystallin, the height of the two major [14]N peaks roughly doubles upon reducing temperature from 25 to 5°C, as for $\gamma_{II}$-crystallin (6), whereas for α-crystallin (35) the increase in the peak heights is much less, ≲15%. (For calf lens homogenates, there is no variation with temperature (see Fig. 1 of reference 33.)

## DISCUSSION

### Low-concentration behavior of $\beta_L$-crystallin

The relatively large value of $\tau_R$ derived from the NMRD data, Fig. 1, which corresponds to ~200 kD for a compact spherical protein in the dilute limit (as estimated from rotational Brownian motion), means that the volume of this ostensibly 60 kD protein is about three times its compact value. (This estimate assumes that BSA is hydrodynamically spherical; as noted above, accounting for asphericity can increase this value ~50%.) This finding of a large hydrodynamic volume for $\beta_L$-crystallin may be attributed to the unusual shape of the solute molecules, much like a square hour-glass or two tetrahedrons attached apex to apex (47). This shape, as noted above, makes the NMRD data consistent with the osmotic pressure data at lower concentrations, which are compatible with a number density of solute particles derived assuming 80 kD for $\beta_L$-crystallin (25) (Kenworthy, Magid, and McIntosh, manuscript in preparation). Interestingly, the only other protein found to be noncompact from NMRD measurements is $\alpha$-crystallin (4, 35), a much larger protein constructed of 20-kD subunits. Even apoferritin, a hollow sphere about the size of $\alpha$-crystallin and assembled from 24 noncovalently associated subunits of 22 kD, appears compact from NMRD measurements (50). Thus, it may be more than coincidental, and related to crystallin function (see below), that $\alpha$- and $\beta_L$-crystallins have large hydrodynamic excluded volumes.

## Midconcentration behavior of $\beta_L$-crystallin

Over the range 10–20% vol/vol, Fig. 2 and Table 1, the NMRD profiles (which arise from Brownian rotation of macromolecular solute) of $\beta_L$-crystallin are those of particles about two-thirds the hydrodynamically equivalent spherical volume of $\alpha$-crystallin, as already noted. These observations can be accounted for by oligomerization, which should not be surprising, given that $\gamma_{II}$-crystallin oligomerizes dramatically (6) and that the major tertiary structural motifs of $\gamma_{II}$-crystallin and $\beta_L$-crystallin are almost identical (47). From NMRD data, solute $\gamma_{II}$-crystallin particles increase in size from ~20 kD to the equivalent of a 300 kD compact protein at 15% vol/vol, whereas $\beta_L$-crystallin becomes the equivalent of ~1,000 kD, threefold larger in equivalent spherical hydrodynamic volume than $\gamma_{II}$-crystallin. However, it should be noted that $\beta_L$-crystallin may be unique among mammalian crystallins because of its unusual molecular shape: its apparent volume, as derived from effective hydrodynamic size, cannot yet (4) be easily related to the (entropic) excluded volume relevant to the computation of osmotic virial coefficients as can, for example, the spherical $\alpha$-crystallin (10).

## High-concentration behavior of $\beta_L$-crystallin

Taken together with the NMRD data for $\alpha$- and $\gamma$-crystallins at high concentrations, from which it was shown that the profiles intersect (35) (much as does the colloid osmotic pressure (10)), the present results indicate that $\beta_L$-crystallin differs from $\gamma_{II}$-crystallin only in that the mean hydrodynamic size of $\beta_L$-crystallin oligomers does not continue to increase with increasing concentration, as does that of $\gamma_{II}$-crystallin.

## An overview of crystallins

The results, Fig. 4, indicate that all mammalian crystallins, as well as chicken lens homogenate (mostly $\delta$-crystallin), display an onset of intermolecular interactions near ~17% protein that, as demonstrated previously (6), does not appear in solutions of proteins other than crystallins until ~30% protein vol/vol, i.e., 41 wt%, (see reference 29). Thus, it is a ready inference, from Fig. 4, that all crystallins (as found for $\alpha$-crystallin (9, 11, 51) and concluded here for $\beta_L$-crystallin) are noncompact in that their effective rotational hydrodynamic volumes per solute particle are two- to threefold greater than calculated for compact spheres of equivalent molecular weights. This explains the onset of intermolecular interactions at a protein concentration as low as one-half the weight-fraction expected, independent of the extent of oligomerization (if any) of solute. The mechanisms underlying the mobile-immobile (i.e., solid-state like) "transition" in crystallins, as exhibited in NMRD profiles, has only recently been clarified (30, 35, 49), and involves changes in the details of nuclear relaxation and transport when Brownian rotation is slower than that of a 50,000 kD sphere (see reference 29). (Indications of both liquid- and solid-state behavior at high concentrations have been reported in off-resonance and cross-polarization high resolution NMR measurements, respectively, of bovine lens homogenates (52). Although it is not clear which crystallins of the homogenates contribute to the NMR signals, the cross-relaxation data do show an increase of solid-state behavior with increased protein concentration. The off-resonance rotating frame results, from which rotational relaxation times are derived, are more questionable, since the interpretation of such data in terms of rotational mobility has been recently questioned (53).) However, despite incomplete theoretical understanding, the phenomenology is clear. One must then ask the reason for such universal behavior among the different crystallins.

It has been pointed out (10) that the same total weight of protein distributed among spherical macromolecules of the same mass, compact in one case and noncompact in another, scatter visible light to different extents. In particular, for solutions of as large a protein as $\alpha$-crystallin, and near physiological concentrations, noncompact solute would give 99% transmission whereas compact solute would give 85% transmission. (The effect is less dramatic for smaller proteins.) The mechanism is straightforward: The less compact the protein, i.e., the "smoother" the spatial variation of protein, the smaller are the Fourier components of the index of refraction fluctuations at the longer visible-light wavelengths that contribute most to scattering.

A disadvantage of less compact solute is that the usual repulsive intermolecular interactions, and the associated increase in colloid osmotic pressure, become large at lower total protein fraction. Oligomerization can offset such osmotic effects (a ready explanation of the greater $\alpha$- to $\gamma$-crystallin content (3:1) of calf lens cortex compared with lens nucleus (2:3) (see Table 1 of reference 9). $\gamma$-crystallin oligomers of various sizes can also fill the voids between the much larger $\alpha$-crystallin molecules, thus augmenting transparency while mitigating osmotic problems.

The total $\beta$-crystallin content of cortex and nucleus is relatively constant, although the relative amounts of $\beta_L$-crystallin and $\beta_H$-crystallin differ substantially (54). $\beta_L$-crystallin, much as $\gamma$-crystallin, can also act as a "filler" between the much larger $\alpha$-crystallin molecules, reducing density fluctuations and thereby improving transparency, but with the opposite effect on osmotic pressure. Osmotic problems (arising either from protein gradients in the lens or from differential composition between the lens and neighboring tissue) can be resolved dynamically by pumping ions, but this requires metabolism and the concommitant requirement of mitochondria and heme chromophores which, in turn, compromises transparency. The delicate balance of protein composition of mammalian eye lens, and its spatial variation, addresses the dual need to maximize transparency and maintain static osmotic equilibria by using three classes of crystallins with specialized densities, shapes, and associative properties. The NMRD behavior of $\beta_H$-crystallin remains to be studied.

Supported in part by NIH grant GM27278 and a Duke University Medical Center Research Grant.

We also acknowledge helpful discussions with Drs. Christine Slingsby and Annette Tardieu.

*Received for publication 3 June and in final form 9 December 1992.*

## REFERENCES

1. Wistow, G., and J. Piatigorsky. 1988. Lens crystallins: the evolution and expression of proteins for a highly specialized tissue. *Annu. Rev. Biochem.* 57:479–504.
2. Piatigorsky, J., and G. Wistow. 1991. The recruitment of crystallins: new functions precede gene duplication. *Science (Wash. DC).* 252:1078–1079.
3. Driessen, H. P. C., B. Bax, C. Slingsby, P. F. Lindley, D. Mahadevan, D. S. Moss, and I. J. Tickle. 1991. Structure of oligomeric $\beta$B2-crystallin: an application of the $T_2$ translation function to an asymmetric unit containing two dimers. *Acta Cryst.* B47:987–997.
4. Koenig, S. H. 1992. Concentration-dependent association of crystallins: implications for protein function and MRI. *Biophys. J.* 61:A139. (Abstr.)
5. Koenig, S. H., C. F. Beaulieu, R. D. Brown III, and M. Spiller. 1989. Protein-protein interactions, conformation change, and the phase transition in $\gamma_{II}$-crystallin solutions. *Invest. Ophthal. Vis. Sci.* 30(Suppl.):265*a*. (Abstr.)
6. Koenig, S. H., C. F. Beaulieu, R. D. Brown III, and M. Spiller. 1990. Oligomerization and conformation change in solutions of calf lens $\gamma_{II}$-crystallin. *Biophys. J.* 57:461–469.
7. Magid, A. D., T. J. McIntosh, and S. A. Simon. 1989. Osmotic pressure of bovine lens crystallins. *Biophys. J.* 55:A21. (Abstr.)
8. Magid, A. D., A. K. Kenworthy, and T. J. McIntosh. 1992. Colloid osmotic pressure of steer crystallins: implications for the origin of the refractive index gradient and transparency of the lens. *Exp. Eye Res.* In press.
9. Vérétout, F., and A. Tardieu. 1989. The protein concentration gradient within eye lens might originate from constant osmotic pressure coupled to differential interactive properties of the protein. *Eur. Biophys. J.* 17:61–68.
10. Vérétout, F., M. Delaye, and A. Tardieu. 1989. Molecular basis of eye lens transparency. Osmotic pressure and X-ray analysis of $\alpha$-crystallin solutions. *J. Mol. Biol.* 205:713–728.
11. Licinio, P., and M. Delaye. 1988. Direct and Hydrodynamic Interactions between $\alpha$-crystallin proteins in dilute colloidal dispersions: a light scattering study. *J. Colloid Interface. Sci.* 123:105–116.
12. Carnahan, N. F., and K. E. Starling. 1969. Equation of state for nonattracting rigid spheres. *J. Chem. Phys.* 51:635–636.
13. Croft, L. R. 1972. Amino acid sequence of gamma-crystallin (fraction II) from calf lens. *Biochem. J.* 128:961–970.
14. Tardieu, A., F. Vérétout, B. Krop, and C. Slingsby. 1992. Protein interactions in the calf eye lens: interactions between $\beta$-crystallins are repulsive whereas in $\gamma$-crystallins they are attractive. *Eur. Biophys. J.* 21:1–12.
15. Zigler, J. S. 1978. Age-related changes in the polypeptide composition of $\beta$-crystallin from bovine lens. *Exp. Eye Res.* 26:537–546.
16. Bloemendal, H., I. Hendriks, and P. Body. 1990. $\beta_H$- and $\beta_L$-crystallins are populations of aggregates. *Exp. Eye Res.* 50:711–3.
17. Slingsby, C., and O. A. Bateman. 1990. Quaternary interactions in eye lens $\beta$-crystallins: basic and acidic subunits of $\beta$-crystallins favor heterologous association. *Biochemistry.* 29:6592–6599.
18. Lapatto, R., V. Nalini, B. Bax, H. Driessen, P. F. Lindley, T. L. Blundell, and C. Slingsby. 1991. High resolution structure of an oligomeric eye lens $\beta$-crystallin. Loops, arches, linkers and interfaces in $\beta$B2 dimer compared to a monomeric $\gamma$-crystallin. *J. Mol. Biol.* 222:1067–1083.
19. Slingsby, C., A. Simpson, A. Ferszt, O. A. Bateman, and V. Nalini. 1992. Molecular interactions in eye lens. *Biochem. Soc. Transactions.* 19:853–858.
20. Zigler, J. S., and J. B. Sidbury. 1973. Structure of calf lens $\beta$-crystallins. *Exp. Eye Res.* 16:207–214.
21. Asselbergs, F. A. M., M. Koopmans, W. J. van Venroolj, and H. Bloemendal. 1979. Improved resolution of calf lens $\beta$-crystallins. *Exp. Eye Res.* 28:223–228.
22. Berbers, G. A. M., O. C. Boerman, H. Bloemendal, and W. W. de Jong. 1982. Primary gene products of bovine beta-crystallin and reassociation behavior of its aggregates. *Eur. J. Biochem.* 128:495–502.
23. Chiou, S. H., P. Azari, M. E. Himmel, H. K. Lin, and W. P. Chang. 1989. Physicochemical characterization of beta-crystallins from bovine lenses: hydrodynamic and aggregation properties. *J. Protein Chem.* 8:19–32.
24. Kenworthy, A. K., and A. D. Magid. 1991. Osmotic pressure measurements of $\beta$-crystallins from bovine lens. *Biophys. J.* 59:A110. (Abstr.)
25. Kenworthy, A. K., T. J. McIntosh, and A. D. Magid. 1992. Ionic strength dependence of the colloid osmotic pressure of bovine lens crystallins. *Biophys. J.* 61:A477. (Abstr.)
26. Prouty, M. S., A. N. Schechter, and V. A. Parsegian. 1985. Chemical potential measurements of deoxyhemoglobin S polymerization. Determination of the phase diagram of an assembling protein. *J. Mol. Biol.* 184:517–528.
27. Koenig, S. H., and W. E. Schillinger. 1969. Nuclear magnetic relaxation dispersion in protein solutions I. Apotransferrin. *J. Biol. Chem.* 244:3283–3289.
28. Hallenga, K., and S. H. Koenig. 1976. Protein rotational relax-

ation as studied by solvent $^1H$ and $^2H$ magnetic relaxation. *Biochemistry.* 15:4255–4264.

29. Koenig, S. H., and R. D. Brown III. 1991. Field-cycling relaxometry of proteins and tissue: Implications for MRI. 1991. *Progr. NMR Spectr.* 22:487–567.
30. Koenig, S. H., R. D. Brown III, and R. Ugolini. 1993. A unified view of relaxation in protein solutions and tissue, including hydration and magnetization transfer. *Magn. Reson. Med.* 29:77–83.
31. Koenig, S. H., R. G. Bryant, K. Hallenga, and G. S. Jacob. 1978. Magnetic cross-relaxation among protons in protein solutions. *Biochemistry.* 17:4348–4358.
32. Beaulieu, C. F., J. I. Clark, R. D. Brown III, M. Spiller, and S. H. Koenig. 1988. Relaxometry of calf lens homogenates, including cross-relaxation by crystallin NH Groups. *Magn. Reson. Med.* 8:45–57.
33. Beaulieu, C. F., R. D. Brown III, J. I. Clark, M. Spiller, and S. H. Koenig. 1989. Relaxometry of lens homogenates II: temperature dependence and comparison with other proteins. *Magn. Reson. Med.* 10:62–72.
34. Beaulieu, C. 1989. Nuclear magnetic resonance studies of lens transparency. UMI Dissertation Information Service, Ann Arbor, MI.
35. Koenig, S. H., R. D. Brown III, M. Spiller, B. Chakrabarti, and A. Pande. 1992. Intermolecular interactions and conformation change in solutions of calf lens $\alpha$-crystallin. *Biophys. J.* 61:776–785.
36. Winter, F., and R. Kimmich. 1982. Spin lattice relaxation of dipole nuclei ($I = 1/2$) coupled to quadrupole nuclei ($S = 1$). *Mol. Phys.* 45:33–49.
37. Winter, F., and R. Kimmich. 1982. NMR field-cycling relaxation spectroscopy of bovine serum albumin, muscle tissue, *micrococcus luteus,* and yeast. $^{14}N\,^1H$ quadrupole dips. *Biochim. Biophys. Acta.* 719:292–298.
38. Koenig, S. H., R. D. Brown III, D. Adams, D. Emerson, and C. G. Harrison. 1984. Magnetic field dependence of $1/T_1$ of protons in tissue. *Invest. Radiol.* 19:76–81.
39. Kimmich, R., F. Winter, W. Nusser, and K.-H. Spohn. 1986. Interactions and fluctuations deduced from proton field-cycling relaxation relaxation spectroscopy of polypeptides, DNA, muscles, and algae. *J. Magn. Reson.* 66:263–282.
40. Koenig, S. H. 1988. Theory of relaxation of mobile water protons by protein NH moieties, with application to rat heart muscle and calf lens homogenates. *Biophys. J.* 53:91–96.
41. Koenig, S. H., and R. D. Brown III. 1987. Relaxometry of tissue. *In* NMR Spectroscopy of Cells and Organisms, Vol. II. R. K. Gupta, editor. CRC Press, Boca Raton, FL. 75–114.
42. Koenig, S. H., and R. D. Brown III. 1985. Relaxation of solvent protons and deuterons by protein-bound $Mn^{2+}$ ions. Theory and experiment for $Mn^{2+}$-concanavalin A. 1984. *J. Magn. Reson.* 61:426–439.
43. Cole, K. S., and R. H. Cole. 1941. Dispersion and absorption in dielectrics. I. Alternating current characteristics. *J. Chem. Phys.* 9:341–351.
44. Woessner, D. E. 1962. Spin relaxation processes in a two-proton system undergoing anisotropic reorientation. *J. Chem. Phys.* 37:647–654.
45. Koenig, S. H. 1975. Brownian motion of an ellipsoid. A correction to Perrins's results. *Biopolymers.* 14:2421–2423.
46. Koenig, S. H. 1980. The dynamics of water-protein interactions: results from measurements of nuclear magnetic relaxation dispersion. *In* Water in Polymers. S. P. Rowland, editor. ACS Symposium Series, Washington, DC. 127:157–176.
47. Bax, B., R. Lapatto, V. Nalini, H. Driessen, P. F. Lindley, D. Mahadevan, T. L. Blundell, and C. Slingsby. 1990. X-ray analysis of $\beta$B2-crystallin and evolution of oligomeric lens proteins. *Nature (Lond.).* 347:776–80.
48. Koenig, S. H., R. D. Brown III, and R. Ugolini. 1993. Magnetization transfer in cross-linked bovine serum albumin solutions at 200 MHz: a model for tissue. *Magn. Reson. Med.* 29:311.
49. Koenig, S. H., R. D. Brown III, A. Pande, and R. Ugolini. 1993. Rotational inhibition and magnetization transfer in $\alpha$-crystallin solutions. *J. Magn. Reson. B.* In press.
50. Koenig, S. H., R. D. Brown III, J. F. Gibson, R. J. Ward, and T. J. Peters. 1986. Relaxometry of ferritin solutions and the influence of the $Fe^{3+}$ core ions. *Magn. Reson. Med.* 3:755–767.
51. Licinio, P., M. Delaye, A. K. Livesey, and L. Léger. 1987. Colloidal dispersions of $\alpha$-crystallin proteins. II. Dynamics: a maximum entropy analysis of photon correlation spectroscopy data. *J. Physique.* 48:1217–1223.
52. Morgan, C. F., T. Schleich, G. H. Caines, and P. N. Farnsworth. 1989. Elucidation of intermediate (mobile) and slow (solidlike) protein motions in bovine lens homogenates by carbon-13 NMR spectroscopy. *Biochemistry.* 28:5065–5074.
53. Brown, R. D. III, and S. H. Koenig. 1992. $1/T_{1\rho}$ and low field $1/T_1$ of tissue water protons arise from magnetization transfer to macromolecular solid-state broadened lines. *Magn. Reson. Med.* 28:145–152.
54. Pierscionek, B., and R. C. Augusteyn. 1988. Protein distribution patterns in concentric layers from single bovine lenses: Changes with development and ageing. *Curr. Eye Res.* 7:11–23.